


Cite this: *RSC Adv.*, 2025, **15**, 1747

## *In situ* generation and conversion of a half-zirconocene catalyst for the synthesis of *N*-acylpyrazoles†

Juan Wu,‡<sup>a</sup> Mingming Yang, ‡<sup>a</sup> Deying Leng, <sup>b</sup> Qiuping Hu, <sup>a</sup> Yanxiu Yao, <sup>c</sup> Huaming Sun<sup>c</sup> and Ziwei Gao \*<sup>ac</sup>

Pyrazoles are an important class of five-membered nitrogen heterocyclic compounds that have been widely used in agriculture and medicine. Exploring their synthesis methods under mild conditions has always been a hot research topic. Herein, a new strategy was developed to enhance the activity of a zirconium metal centre for the synthesis of *N*-acylpyrazole derivatives using  $\text{Cp}_2\text{ZrCl}_2$  as a pre-catalyst.  $\text{Cp}_2\text{ZrCl}_2$  was activated *in situ* within the catalytic system through cyclopentadienyl ring dissociation, leading to the formation of an activated species,  $[\text{CpZrCl}(\text{acac})_2]$ . The new approach demonstrates broad substrate scope under mild reaction conditions, leading to formation of (3,5-dimethyl-1*H*-pyrazol-1-yl)(phenyl)methanones with yields of up to 97%.

Received 14th November 2024  
Accepted 7th January 2025

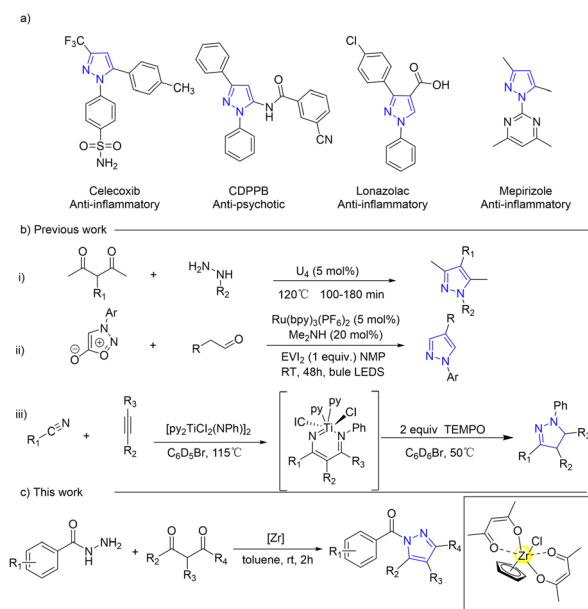
DOI: 10.1039/d4ra08083a  
rsc.li/rsc-advances

## Introduction

Pyrazoles, a significant class of five-membered nitrogen heterocyclic compounds, serve as versatile building blocks<sup>1–3</sup> and crucial intermediates<sup>4,5</sup> in organic synthesis. They exhibit a wide range of pharmaceutical activities and are extensively studied in medical research<sup>6–9</sup> for their anti-tubercular, anti-cancer,<sup>10</sup> anti-depressant, anti-bacterial,<sup>11,12</sup> and anti-parkinsonism activities (Scheme 1a). Several methods, such as cyclocondensation of hydrazine and its derivatives with carbonyl systems,<sup>13–18</sup> dipolar cycloadditions,<sup>19–23</sup> and multi-component reactions,<sup>24,25</sup> have been employed in the development of pyrazoles (Scheme 1b). However, certain existing synthetic approaches for pyrazole synthesis necessitate expensive metal catalysts, harsh reaction conditions, and inconvenient operations as well as yield low product quantities. These limitations impose constraints on the practicality of these reactions, thereby necessitating the establishment of convenient, mild, high-yielding methods that employ cost-effective and less toxic reagents for *N*-acylpyrazole synthesis.

The use of tetravalent IVB Lewis acid catalysts coordinated with cyclopentadienyl (Cp), such as titanocene<sup>26–32</sup> and

zirconocene,<sup>33–37</sup> has been demonstrated to be more diverse, efficient, and practical for C–C<sup>38–43</sup> and C–N<sup>44–47</sup> formation reactions. This is attributed to their cost-effectiveness,<sup>48</sup> low toxicity,<sup>49</sup> high stability,<sup>50</sup> tunable Lewis acidity,<sup>51,52</sup> and high coordination number.<sup>53–57</sup> By incorporating the Cp ligand into the catalyst system, the requirement for stringent anhydrous conditions can also be eliminated due to its less electron deficiency and steric hindrance, which provides a hydrophobic



**Scheme 1** Structures of significant pyrazoles and novel synthetic routes for *N*-acylpyrazole.

<sup>a</sup>School of Chemistry and Chemical Engineering, Yan'an University, Yan'an 716000, P.R. China. E-mail: mmyang@yau.edu.cn

<sup>b</sup>School of Physics and Electronic Information, Yan'an University, Yan'an 716000, P.R. China

<sup>c</sup>Key Laboratory of Applied Surface and Colloid Chemistry, MOE, School of Chemistry and Chemical Engineering, Shaanxi Normal University, Xi'an 710119, P.R. China. E-mail: zwgao@snnu.edu.cn

† Electronic supplementary information (ESI) available. See DOI: <https://doi.org/10.1039/d4ra08083a>

‡ J. Wu and M. Yang contributed equally to this work.



domain for protecting the Lewis acid centre against water.<sup>58–60</sup> However, increased catalyst stability comes at the expense of catalytic activity. The development of a titanocene or zirconocene catalyst with a single Cp ligand is advisable in order to maintain the original catalytic stability and further enhance its catalytic performance.<sup>61,62</sup> Nowadays, the synthesis of these catalysts typically involves the use of precursors such as  $\text{Cp}_2\text{ZrCl}_3$ <sup>63,64</sup> and  $\text{CpTiCl}_3$ ,<sup>65–68</sup> which require intricate procedures and a stringent anhydrous and oxygen-free environment, in addition to being costly. The establishment of an *in situ*, convenient, and mild conversion method for a half-zirconocene catalyst is therefore imperative to enable its direct application in catalytic reactions. Additionally, these diverse coordination modes between zirconium and both the ligand<sup>69–71</sup> and substrate<sup>72–74</sup> facilitate facile capture of adduct products and thereby enable comprehensive investigation into catalyst–substrate interaction.

Herein, we present an *in situ* acetylacetone-coordinated half-zirconocene complex and its catalytic role in the synthesis of *N*-acylpyrazoles, as depicted in Scheme 1c. The evidence from *in situ* ESI(+)–MS and  $^1\text{H}$  NMR experiments elucidated the interaction between the zirconium centre and substrates. The catalyst effectively facilitated the synthesis of pyrazoles, achieving a remarkable yield of 97% under mild, low catalyst loading, non-anhydrous and non-anaerobic conditions.

## Results and discussion

Our experimental optimization for *N*-acylpyrazole synthesis commenced with benzoyl hydrazine (**1a**) and acetylacetone (acac) (**2a**), resulting in the formation of two products, namely, *N*-acylpyrazole (**3a**) and 5-hydroxy-dihydropyrazole (**5a**). The reaction was conducted at room temperature for 2 hours in toluene solvent using 5 mol% of  $\text{Cp}_2\text{ZrCl}_2$  as a pre-catalyst, leading to the desired *N*-acylpyrazole **3a** ((3,5-dimethyl-1*H*-pyrazol-1-yl)(phenyl)methanone) with a high yield of 97% (Table 1, entry 1). The control experiment confirmed the essential role of zirconium catalyst in preventing the undesirable generation of compound **5a** (entry 2). Initially, various solvents were evaluated employing  $\text{Cp}_2\text{ZrCl}_2$  as a pre-catalyst; their results are presented in entries 3–8 of Table 1. DMSO provided a yield of only 47% while THF, DMF, acetonitrile, EtOH and  $\text{CH}_2\text{Cl}_2$  exhibited similar yields, ranging from 80% to 90%. Consequently, toluene was identified as the optimal choice due to its superior yield up to 97%. Subsequently, several catalysts were examined (entries 9–18). Considering that oxygen within acetylacetone readily interacts with the zirconium metal centre,  $\text{ZrCl}_4$  was initially assessed due to its easily breakable Zr–Cl bonds, resulting in an 88% yield. However, the presence of  $\text{Zr}(\text{OH})_4$  failed to produce desired product **3a** while yielding only 22% of compound **5a**, possibly due to the inability of stable Zr–OH ligand to be replaced by acetylacetone.  $\text{Zr}(\text{OAc})_2$  yielded only 83% of compound **5a** without any desired product formation. Acetylacetone zirconium was introduced as a contrasting catalyst to the *in situ* coordinating complex, resulting in only 22% yield of **5a**.  $\text{CpZrCl}_3$  was employed as a formed half-zirconocene catalyst, giving 90% yield, consistent with

Table 1 Solvent and catalyst effect in the reaction of benzoyl hydrazine and acetylacetone<sup>a</sup>

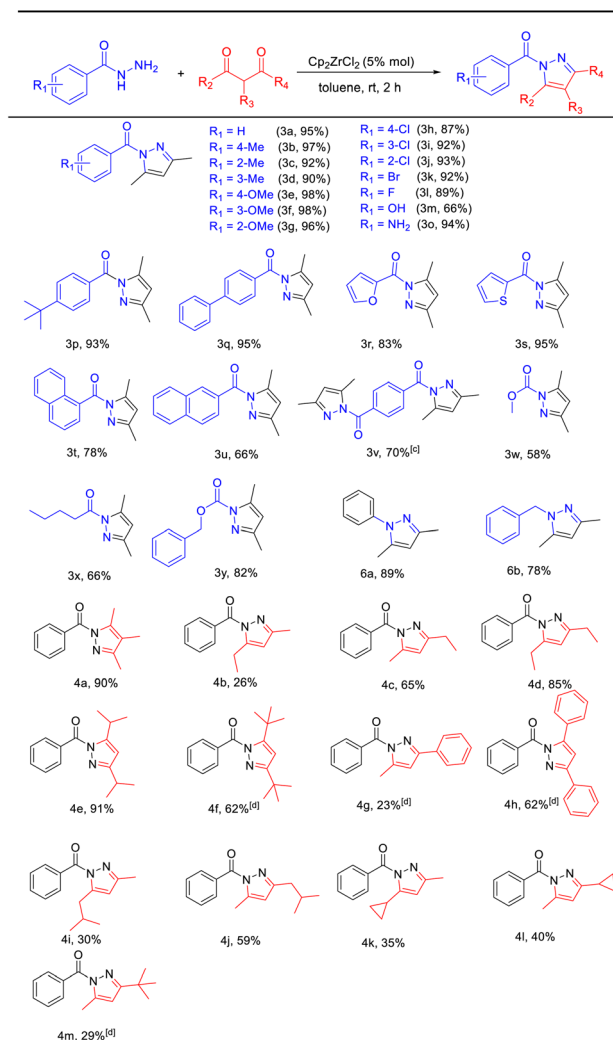
Entry	Catalyst	Solvent	Yield <sup>b</sup> (%)	
			Product <b>3a</b>	Product <b>5a</b>
1	$\text{Cp}_2\text{ZrCl}_2$	Toluene	97	—
2	—	Toluene	—	76
3	$\text{Cp}_2\text{ZrCl}_2$	DMSO	47	—
4	$\text{Cp}_2\text{ZrCl}_2$	THF	82	—
5	$\text{Cp}_2\text{ZrCl}_2$	DMF	80	—
6	$\text{Cp}_2\text{ZrCl}_2$	$\text{CH}_3\text{CN}$	81	—
7	$\text{Cp}_2\text{ZrCl}_2$	$\text{CH}_2\text{Cl}_2$	87	—
8	$\text{Cp}_2\text{ZrCl}_2$	EtOH	90	—
9	$\text{ZrCl}_4$	Toluene	88	—
10	$\text{Zr}(\text{OH})_4$	Toluene	—	22
11	$\text{Zr}(\text{OAc})_2$	Toluene	—	83
12	$\text{Zr}(\text{O}_2\text{C}_5\text{H}_7)_4$	Toluene	—	22
13	$\text{CpZrCl}_3$	Toluene	90	—
14	$\text{FeCl}_3 \cdot 6\text{H}_2\text{O}$	Toluene	74	—
15	$\text{CuCl}_2 \cdot 2\text{H}_2\text{O}$	Toluene	36	—
16	PTSA	Toluene	—	—
17	Sulfamic acid	Toluene	32	—
18	Camphor sulfonic acid	Toluene	79	—

<sup>a</sup> 0.5 mmol of benzoyl hydrazine, 0.5 mmol of acetylacetone and 5% of the catalyst in 0.5 mL solvent at room temperature for 2 h. <sup>b</sup> Yield of  $^1\text{H}$  NMR.

$\text{Cp}_2\text{ZrCl}_2$ . When  $\text{FeCl}_3 \cdot 6\text{H}_2\text{O}$  and  $\text{CuCl}_2 \cdot 2\text{H}_2\text{O}$  were used as Lewis acid catalysts, the desired products were obtained with yields of 74% and 36%, respectively. Several mild acids, including PTSA, sulfamic acid and camphor sulfonic acid, were introduced as alternatives to the Zr catalyst. Consequently, the yields of the target product were 0%, 32% and 79%, respectively.

With the optimized conditions established, the substrate scope was explored by reacting various benzoyl hydrazines with acetylacetone. The reactivity of various substituted benzoyl hydrazines was examined and is summarized in Table 2. Electron-donating groups such as –Me and –OMe gave *N*-acylpyrazole yields in the range of 90–98% (**3b**–**3g**), while electron-withdrawing halogen groups (–F, –Cl, –Br) produced the desired products with 87–93% yields (**3h**–**3l**). 66% yield (**3m**) for the benzoyl hydrazine with –OH substitution was obtained, which can be attributed to the facile coordination of the oxygen atom in the hydroxyl group with the zirconium metal centre, thereby causing catalyst poisoning and rendering it inactive. The amino-substituted benzoyl hydrazine underwent a reaction with acetylacetone, leading to the formation of two distinct products. One of these products was the desired compound **3o**, while the other product **3n** exhibited an imine structure resulting from subsequent interaction between compound **3o** and another molecule of acetylacetone. The reaction between *p*-*tert*-butyl and *p*-phenyl-substituted benzoyl hydrazine resulted in a product yield of 93% for compound **3p** and 95% for



Table 2 Cyclization of benzoyl hydrazine and acetylacetone.<sup>a,b</sup>

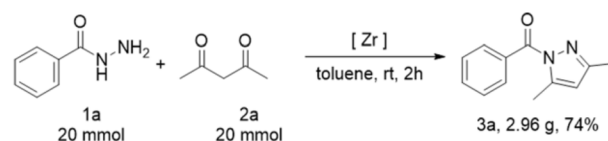
<sup>a</sup> 0.5 mmol of benzoyl hydrazine, 0.5 mmol of acetylacetone, 5% of  $\text{Cp}_2\text{ZrCl}_2$  in 0.5 mL solvent at room temperature for 2 h. <sup>b</sup> Yield of the isolated product. <sup>c</sup> 1.0 mmol acetylacetone was used. <sup>d</sup> 120 °C for 12 h.

compound **3q**, respectively. Heterocyclic substituted substrates including furyl-, thiienyl-, 1-naphthyl-, and 2-naphthyl- exhibited favorable yields of 83%, 95%, 78%, and 66%, respectively (**3r**–**3u**). Upon the introduction of terephthalic dihydrazide, each of the two hydrazide groups underwent a reaction with one molecule of acetylacetone. Consequently, we increased the amount of acetylacetone to 2 equivalents in order to obtain a product featuring two pyrazole rings, yielding 70% (**3v**). In the absence of aromatic ring influence (**3w**–**3y**), the corresponding *N*-acylpyrazoles were obtained with moderate yields ranging from 58% to 82%. Simple hydrazine examples, including phenylhydrazine and benzylhydrazine, were also evaluated under the optimized conditions. The reactions gave 89% yield for compound **6a** and 78% for compound **6b**. The impact of changes in  $\beta$ -diketone derivatives on the reaction was subsequently investigated, resulting in excellent yields ranging from

85% to 91% (**4a**, **4d**, **4e**). The introduction of 2,4-hexanedione led to the formation of two distinct structures, namely, **4b** and **4c**, due to variations in the order of reaction between the 2-carbonyl and 4-carbonyl groups. These findings suggest that the generation of structure **4c** is more favorable. Similarly, 6-methylheptane-2,4-dione resulted in the formation of compounds **4i** and **4j** with yields of 30% and 59%, respectively. Additionally, 1-cyclopropyl-1,3-butandione produced the corresponding *N*-acylpyrazoles **4k** and **4l**, yielding 35% and 40%, respectively. When the substituent of  $\beta$ -diketone is changed to *tert*-butyl or phenyl, the conversion of enone may be hindered by site-blocking effects, necessitating an increase in reaction temperature and time to achieve moderate yields of the target products (**4f**–**4h**). Dipivaloylmethane affords the product with a yield of 62% (**4f**). Benzoylacetone only yields 23% of the desired product (**4g**). Dibenzoylmethane provides the corresponding *N*-acylpyrazole with a yield of 62% (**4h**). The reaction of 5,5-dimethylhexane-2,4-dione results in the formation of compound **4m** with a yield of 29%.

The scalability of this half-zirconocene catalytic system was assessed by conducting a 20 mmol scale reaction in a reaction tube under standard conditions (Scheme 2). The reaction between **1a** and **2a** yielded the desired product (3,5-dimethyl-1*H*-pyrazol-1-yl)-(phenyl)methanone with a yield of 74%.

To elucidate the activation mechanism of the reaction between acetylacetone and benzoyl hydrazine in the presence of  $\text{Cp}_2\text{ZrCl}_2$ , <sup>1</sup>H NMR titration experiments were conducted (Fig. 1a). The gradual addition of acetylacetone and benzoyl hydrazine to a solution of  $\text{Cp}_2\text{ZrCl}_2$  resulted in changes in the Cp signal, as detected in the <sup>1</sup>H NMR spectra, which can be attributed to the transformation of zirconocene species. The addition of acetylacetone alone induced a minor new signal at  $\delta$  6.29 ppm (●), indicating coordination between  $\text{Cp}_2\text{Zr}$  and acetylacetone. Upon further addition of benzoyl hydrazine, the peak corresponding to  $\text{Cp}_2\text{ZrCl}_2$  rapidly vanished, while the immediate appearance of a new signal at  $\delta$  6.44 ppm (▲) suggested that conversion had occurred from  $\text{Cp}_2\text{ZrCl}_2$  to a novel zirconium species inconsistent with direct coordination between  $\text{Cp}_2\text{ZrCl}_2$  and acetylacetone. The chemical conversion of  $\text{Cp}_2\text{ZrCl}_2$  might be attributed to the induced effect of benzoyl hydrazine, which not only served as the reaction substrate but also played a crucial role in removing one Cp ligand. In addition to the change in the characteristic hydrogen of Cp ligand, the newly generated peak at  $\delta$  6.13 ppm (✚) gradually increased during the progression of the reaction. This peak is assigned to the alkene hydrogen in the enol structure after acetylacetone coordinates with zirconium. As shown in Fig. 1b, there is a proton number ratio of 2:5 for acetylacetone ( $\text{H}_b$ ) and Cp



Scheme 2 Reaction scale-up.



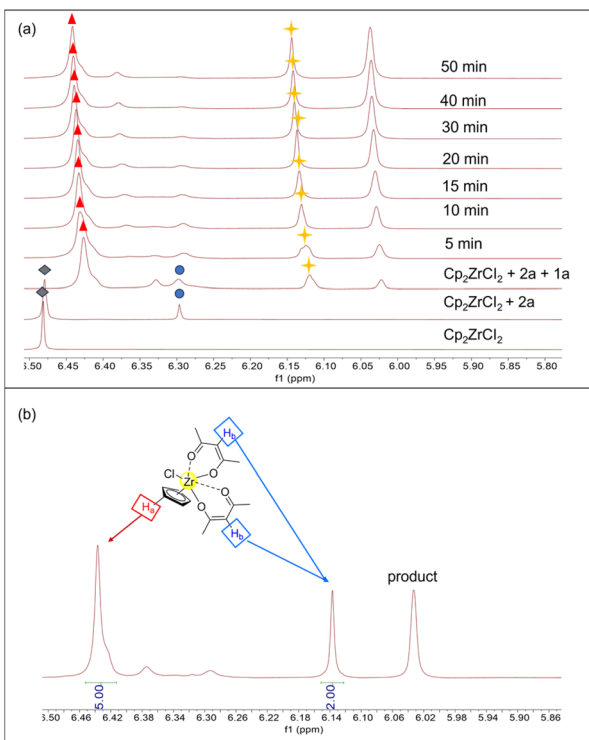


Fig. 1 (a) 400 MHz  $^1\text{H}$  NMR titration experiments. 6.48 ppm [ $\text{Cp}_2\text{ZrCl}_2$ ]; 6.29 ppm [ $\text{Cp}_2\text{ZrCl}(\text{acac})$ ]; 6.44 ppm and 6.13 ppm [ $\text{Cp}_2\text{ZrCl}(\text{acac})_2$ ]. (b) Proton number ratio for acetylacetone ( $\text{H}_\text{b}$ ) and the Cp ligand ( $\text{H}_\text{a}$ ).

ligand ( $\text{H}_\text{a}$ ), indicating that the ligand ratio for acetylacetone and Cp is 2 : 1 in zirconocene catalytic species (more proton number ratio shown in Fig. S8†). The experimental results indicate that the structure of the catalyst possesses a zirconium metal centre coordinated with two acetylacetone molecules, as depicted in Fig. 1b.

The structure of the real catalytic species was further determined through *in situ* ESI(+)–MS experiments, providing insights into potential reaction mechanisms by capturing

several reaction intermediates in the ESI-MS spectra (Fig. 2). The dominant signal at an  $m/z$  value of 353.0321 is attributed to **Int-II**, where two acetylacetone ligands and one Cp ligand are coordinated to the zirconium metal centre. The other major peak, with an  $m/z$  value of 471.0852, corresponds to the compound formed by the coordination of a zirconium centre with an acetylacetone, a Cp ligand, and an imide structure, resulting from the reaction of acetylacetone and imine (**Int-IV**). This peak also arises from a product where the zirconium centre is coordinated with an acetylacetone, a Cp ligand, and an undehydrated intermediate (**Int-V**). The signal at an  $m/z$  value of 489.0962 corresponds to the intermediate structure **Int-III**, which is formed through the coordination of a half-zirconocene with an acetylacetone and the nucleophilic addition of acetylacetone to benzoyl hydrazine. The analysis of these three main peaks reveals that the initial step involves the reaction between acetylacetone and the catalyst, followed by the subsequent reaction between benzoyl hydrazine and acetylacetone. The overall reaction occurs with the participation of the catalytic species. Fig. 2 also illustrates additional peaks that can be identified, facilitating speculation on the catalytic process. The  $m/z$  value of 437.0799 corresponds to **Int-VII**, which consists of two Cp ligands and an imide intermediate structure connected to the zirconium centre. The presence of **Int-VII** indicates that the process of Cp ligand removal has not been completed, which corresponds to the gradual disappearance of the signal at  $\delta$  6.29 ppm (●) in the  $^1\text{H}$  NMR titration experiments. **Int-VIII**, with a mass–charge ratio of  $m/z$  589.1395, comprises one Cp ligand and two undehydrated intermediates connected to zirconium. The peak at  $m/z$  689.1917 corresponds to the intermediate structure **Int-IX**, which bears two undehydrated hydroxy-dihydropyrazole and an acetylacetone. The structures **Int-VIII** and **Int-IX** illustrate that the catalyst possesses the ability to incorporate multiple substrates at a single half-zirconocene catalytic centre, thereby enabling simultaneous catalysis of two or even three molecular reactions during the catalytic process. ESI-MS analysis reveals that  $\text{Cp}_2\text{ZrCl}_2$  undergoes Cp ligand dissociation during catalysis, while the presence of acetylacetone in a coordinated form<sup>69,70</sup> significantly enhances the reaction rate.

After carefully considering the aforementioned  $^1\text{H}$  NMR titration experiments, control experiment results, and ESI-MS analysis collectively, a plausible mechanism for the synthesis of (3,5-dimethyl-1*H*-pyrazol-1-yl)(phenyl)methanone derivatives is proposed (Scheme 3). Initially, benzoyl hydrazine promotes the pre-catalyst  $\text{Cp}_2\text{ZrCl}_2$  to remove Cp ligand and coordinate with two acetylacetone ligands, forming the catalytic species [ $\text{Cp}_2\text{ZrCl}(\text{acac})_2$ ]. Then, the primary amine on benzoyl hydrazine undergoes nucleophilic addition to attack acetylacetone and generate intermediate **III**. This intermediate then proceeds to eliminate a molecule of water and form imine intermediate **IV**. Subsequently, the enol carbon in the imine intermediate **IV** undergoes nucleophilic attack by the secondary amine of benzoyl hydrazine, resulting in the formation of *N,O*-acetal intermediate **V**. Finally, under the facilitation of the half-zirconocene centre, ligand dissociation occurs to release *N,O*-acetal and facilitate its dehydration, enabling the formation of target compound (3,5-

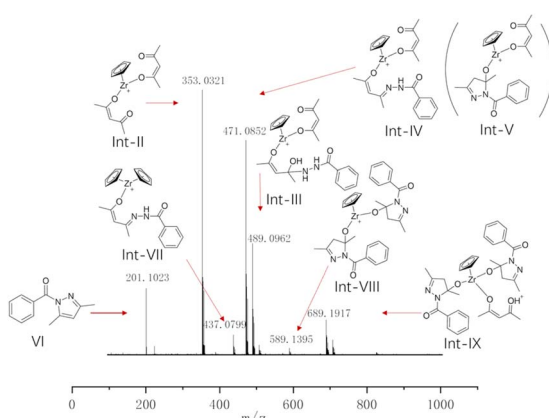
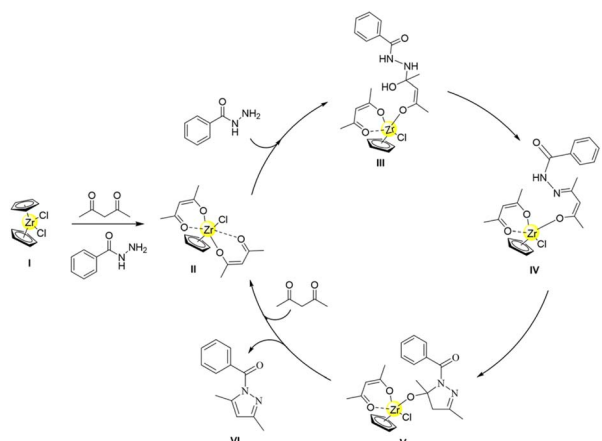


Fig. 2 ESI-MS analysis for the synthesis of *N*-acylpyrazole under standard conditions.



**Scheme 3** Plausible mechanism for the synthesis of (3,5-dimethyl-1*H*-pyrazol-1-yl)(phenyl)methanone catalyzed by *in situ* formed half-zirconocene.

dimethyl-1*H*-pyrazol-1-yl)(phenyl)methanone while regenerating the catalyst species.

## Experimental

### General procedure for synthesis of compound 3a

A representative example of the preparation of (3,5-dimethyl-1*H*-pyrazol-1-yl)(phenyl)methanone (**3a**) is described as follows. The reactants, acetylacetone (50.06 mg, 0.5 mmol), benzoyl hydrazine (68.08 mg, 0.5 mmol),  $\text{Cp}_2\text{ZrCl}_2$  (7.45 mg, 0.025 mmol), and toluene (0.5 mL), were combined in a reactor to establish the reaction system. The reaction was carried out under magnetic stirring at room temperature for 2 hours. Upon completion of the reaction, as confirmed by TLC analysis, the reaction mixture was subjected to silica gel flash column chromatography using an eluent mixture of petroleum ether and EtOAc in a ratio of 10 : 1 to yield the desired product **3a** (97 mg) as a yellow liquid with a yield of 97%.

## Conclusions

In conclusion, the development of an efficient catalytic system that facilitates the condensation and cyclization reaction between benzoyl hydrazine and acetylacetone has been achieved. This system involved the *in situ* formation of half-zirconocene using  $\text{Cp}_2\text{ZrCl}_2$  as a pre-catalyst. Under mild conditions, high yields of *N*-acylpyrazoles were obtained with as low as 5%  $\text{Cp}_2\text{ZrCl}_2$  catalyst loading. Mechanistic studies, including  $^1\text{H}$  NMR, ESI(+)-MS analyses, and control experiments, revealed that the coordination of  $\text{Cp}_2\text{ZrCl}_2$  during the reaction led to the generation of the catalytically active species. The detection of half-zirconocene-based catalyst–substrate adducts by ESI-MS elucidated the process of catalyst–substrate interaction.

## Data availability

The data supporting this article have been included as part of the ESI.†

## Conflicts of interest

There are no conflicts to declare.

## Acknowledgements

The authors acknowledge financial support from the National Natural Science Foundation of China (21771122), the Start-up Funds for the PhD of Yan'an University (YAU202407432, YAU202407402), the Fundamental Research Funds for the Central Universities (GK202103027) and the Key Research and Development Project of Shaanxi Province (2021GY-308).

## References

- 1 F. Franco, S. Meninno, M. Benaglia and A. Lattanzi, *Chem. Commun.*, 2020, **56**, 3073–3076.
- 2 Y. Grell, X. Xie, S. I. Ivlev and E. Meggers, *ACS Catal.*, 2021, **11**, 11396–11406.
- 3 K. Otrubova, S. Chatterjee, S. Ghimire, B. F. Cravatt and D. L. Boger, *Bioorg. Med. Chem.*, 2019, **27**, 1693–1703.
- 4 J. Nandi, M. Z. Vaughan, A. L. Sandoval, J. M. Paolillo and N. E. Leadbeater, *J. Org. Chem.*, 2020, **85**, 9219–9229.
- 5 C. Volpe, S. Meninno, G. Mirra, J. Overgaard, A. Capobianco and A. Lattanzi, *Org. Lett.*, 2019, **21**, 5305–5309.
- 6 M. H. Baren, S. A. Ibrahim, M. M. Al-Rooqi, S. A. Ahmed, M. M. El-Gamil and H. A. Hekal, *Sci. Rep.*, 2023, **13**, 14680.
- 7 J. Dwivedi, S. Sharma, S. Jain and A. Singh, *Mini-Rev. Med. Chem.*, 2018, **18**, 918–947.
- 8 V. Kumar, K. Kaur, G. K. Gupta, A. K. Gupta and S. Kumar, *Recent Pat. Inflammation Allergy Drug Discovery*, 2013, **7**, 124–134.
- 9 L.-P. Mo and Z.-H. Zhang, *Curr. Org. Chem.*, 2011, **15**, 3800–3823.
- 10 Y. Zhang, C. Wu, N. Zhang, R. Fan, Y. Ye and J. Xu, *Int. J. Mol. Sci.*, 2023, **24**, 12724.
- 11 R. T. Iminov, A. V. Mashkov, I. I. Vyzir, B. A. Chalyk, A. V. Tverdokhlebov, P. K. Mykhailiuk, L. N. Babichenko, A. A. Tolmachev, Y. M. Volovenko and A. Biitseva, *Eur. J. Org. Chem.*, 2015, **2015**, 886–891.
- 12 S. Shahbazi, M. A. Ghasemzadeh, P. Shakib, M. R. Zolfaghari and M. Bahmani, *Polyhedron*, 2019, **170**, 172–179.
- 13 Y. R. Girish, K. S. S. Kumar, H. S. Manasa and S. Shashikanth, *J. Chin. Chem. Soc.*, 2014, **61**, 1175–1179.
- 14 Y.-F. Liu, K. Li, H.-Y. Lian, X.-J. Chen, X.-L. Zhang and G.-P. Yang, *Inorg. Chem.*, 2022, **61**, 20358–20364.
- 15 J. P. Raj, D. Gangaprasad, K. Karthikeyan, R. Rengasamy, M. Kesavan, M. Venkateswarulu, M. Vajjiravel and J. Elangovan, *Tetrahedron Lett.*, 2018, **59**, 4462–4465.
- 16 M. Stephan, J. Panther, F. Wilbert, P. Ozog and T. J. Müller, *Eur. J. Org. Chem.*, 2020, **2020**, 2086–2092.
- 17 M. A. Topchiy, D. A. Zharkova, A. F. Asachenko, V. M. Muzalevskiy, V. A. Chertkov, V. G. Nenajdenko and M. S. Nechaev, *Eur. J. Org. Chem.*, 2018, **2018**, 3750–3755.
- 18 G. Yang, Y. Liu, X. Lin, B. Ming, K. Li and C. Hu, *Chin. Chem. Lett.*, 2022, **33**, 354–357.



19 C. P. Lakeland, D. W. Watson and J. P. Harrity, *Chem.-Eur. J.*, 2020, **26**, 155–159.

20 K. Kula, A. Kącka-Zych, A. Łapczuk-Krygier, Z. Wzorek, A. K. Nowak and R. Jasiński, *Molecules*, 2021, **26**, 1364.

21 K. Kula, A. Łapczuk, M. Sadowski, J. Kras, K. Zawadzińska, O. M. Demchuk, G. K. Gaurav, A. Wróblewska and R. Jasiński, *Molecules*, 2022, **27**, 8409.

22 M. S. Ledovskaya, V. V. Voronin, M. V. Polynski, A. N. Lebedev and V. P. Ananikov, *Eur. J. Org. Chem.*, 2020, **2020**, 4571–4580.

23 P. Zhao, Z. Zeng, X. Feng and X. Liu, *Chin. Chem. Lett.*, 2021, **32**, 132–135.

24 G. Mali, B. A. Shaikh, S. Garg, A. Kumar, S. Bhattacharyya, R. D. Erande and A. V. Chate, *ACS Omega*, 2021, **6**, 30734–30742.

25 A. J. Pearce, R. P. Harkins, B. R. Reiner, A. C. Wotal, R. J. Dunscomb and I. A. Tonks, *J. Am. Chem. Soc.*, 2020, **142**, 4390–4399.

26 M. Heinz, G. Weiss, G. Shizgal, A. Panfilova and A. Gansäuer, *Angew. Chem., Int. Ed.*, 2023, **62**, e202308680.

27 F. Mühlhaus, H. Weißbarth, T. Dahmen, G. Schnakenburg and A. Gansäuer, *Angew. Chem.*, 2019, **131**, 14346–14350.

28 T. Oswald, T. Gelert, C. Lasar, M. Schmidtmann, T. Klüner and R. Beckhaus, *Angew. Chem., Int. Ed.*, 2017, **56**, 12297–12301.

29 Y. Q. Zhang, V. Jakoby, K. Stainer, A. Schmer, S. Klare, M. Bauer, S. Grimme, J. M. Cuerva and A. Gansäuer, *Angew. Chem.*, 2016, **128**, 1546–1550.

30 Z. Zhang, R. B. Richrath and A. Gansäuer, *ACS Catal.*, 2019, **9**, 3208–3212.

31 Z. Zhang, D. Slak, T. Krebs, M. Leuschner, N. Schmickler, E. Kuchuk, J. Schmidt, L. I. Domenianni, J. B. Kleine Büning and S. Grimme, *J. Am. Chem. Soc.*, 2023, **145**, 26667–26677.

32 E. Le Roux, *Coord. Chem. Rev.*, 2016, **306**, 65–85.

33 M. Fischer, M. Jaugstetter, R. Schaper, M. Schmidtmann and R. Beckhaus, *Eur. J. Inorg. Chem.*, 2018, **2018**, 5146–5159.

34 R. A. Kehner, M. C. Hewitt and L. Bayeh-Romero, *ACS Catal.*, 2022, **12**, 1758–1763.

35 R. A. Kehner, G. Zhang and L. Bayeh-Romero, *J. Am. Chem. Soc.*, 2023, **145**, 4921–4927.

36 D. J. Mindiola, L. A. Watson, K. Meyer and G. L. Hillhouse, *Organometallics*, 2014, **33**, 2760–2769.

37 N. Romero, Q. Dufrois, L. Vendier, C. Dinoi and M. Etienne, *Chem.-Eur. J.*, 2017, **23**, 15766–15774.

38 R. R. Aysin, M. V. Andreev, V. S. Bogdanov, S. S. Bukalov, A. A. Korlyukov, P. V. Dorovatovskii and V. V. Burlakov, *Organometallics*, 2021, **40**, 1344–1350.

39 M. Reiß, F. Reiß, A. Spannenberg, P. Arndt and T. Beweries, *Organometallics*, 2018, **37**, 4415–4423.

40 N. Romero, Q. Dufrois, N. Crespo, A. Pujol, L. Vendier and M. Etienne, *Organometallics*, 2020, **39**, 2245–2256.

41 Y. Q. Zhang, E. Vogelsang, Z. W. Qu, S. Grimme and A. Gansäuer, *Angew. Chem., Int. Ed.*, 2017, **56**, 12654–12657.

42 Z. Zhang, J. B. Stückrath, S. Grimme and A. Gansäuer, *Angew. Chem., Int. Ed.*, 2021, **60**, 14339–14344.

43 S. Xu and E. I. Negishi, *Acc. Chem. Res.*, 2016, **49**, 2158–2168.

44 Y. Luo, H. Sun, W. Zhang, X. Wang, S. Xu, G. Zhang, Y. Jian and Z. Gao, *RSC Adv.*, 2017, **7**, 28616–28625.

45 Y. Luo, Y. Wu, Y. Wang, H. Sun, Z. Xie, W. Zhang and Z. Gao, *RSC Adv.*, 2016, **6**, 66074–66077.

46 M. Yang, Y. Jian, W. Zhang, H. Sun, G. Zhang, Y. Wang and Z. Gao, *RSC Adv.*, 2021, **11**, 38889–38893.

47 S. Zheng, Y. Jian, S. Xu, Y. Wu, H. Sun, G. Zhang, W. Zhang and Z. Gao, *RSC Adv.*, 2018, **8**, 8657–8661.

48 A. S. Singh, D. R. Naikwadi, K. Ravi and A. V. Biradar, *Mol. Catal.*, 2022, **521**, 112189.

49 A. L. Odom and T. J. McDaniel, *Acc. Chem. Res.*, 2015, **48**, 2822–2833.

50 J. Wang, X. Chen, X. Wang, W.-Q. Zhang, H.-M. Sun, G.-F. Zhang, Y. Wu and Z.-W. Gao, *Transit. Met. Chem.*, 2016, **41**, 731–738.

51 X. Wang, Z. H. Wang, G. Zhang, W. Zhang, Y. Wu and Z. Gao, *Eur. J. Org. Chem.*, 2015, **2016**, 502–507.

52 Y. Wang, Y. Jian, Y. Wu, H. Sun, G. Zhang, W. Zhang and Z. Gao, *Appl. Organomet. Chem.*, 2019, **33**, e4925.

53 R. J. Burford, A. Yeo and M. D. Fryzuk, *Coord. Chem. Rev.*, 2017, **334**, 84–99.

54 S. C. Gagieva, V. A. Tuskaev, D. A. Kurmaev, N. A. Kolosov, A. O. Borissova and B. M. Bulychev, *J. Organomet. Chem.*, 2015, **793**, 155–159.

55 K. Nikoofar and Z. Khademi, *Res. Chem. Intermed.*, 2016, **42**, 3929–3977.

56 A. D. Schwarz, K. R. Herbert, C. Paniagua and P. Mountford, *Organometallics*, 2010, **29**, 4171–4188.

57 Z.-H. Zhang and T.-S. Li, *Curr. Org. Chem.*, 2009, **13**, 1–30.

58 Y. Wu, C. Chen, G. Jia, X. Zhu, H. Sun, G. Zhang, W. Zhang and Z. Gao, *Chem.-Eur. J.*, 2014, **20**, 8530–8535.

59 Y. Wu, X. Wang, Y. Luo, J. Wang, Y. Jian, H. Sun, G. Zhang, W. Zhang and Z. Gao, *RSC Adv.*, 2016, **6**, 15298–15303.

60 M. Yang, Y. Wang, Y. Jian, D. Leng, W. Zhang, G. Zhang, H. Sun and Z. Gao, *Mol. Catal.*, 2020, **498**, 111247.

61 C. Redshaw and Y. Tang, *Chem. Soc. Rev.*, 2012, **41**, 4484–4510.

62 J. Klosin, P. P. Fontaine and R. Figueroa, *Acc. Chem. Res.*, 2015, **48**, 2004–2016.

63 G. Alesso, V. Tabernero and T. Cuenca, *J. Organomet. Chem.*, 2012, **717**, 202–210.

64 H. Dialer, K. Polborn, W. Ponikwar, K. Sünkel and W. Beck, *Chem.-Eur. J.*, 2002, **8**, 691–699.

65 W. Zhao, Q. Yan, K. Tsutsumi and K. Nomura, *Organometallics*, 2016, **35**, 1895–1905.

66 J. Yi, N. Nakatani, N. Tomotsu, K. Nomura and M. Hada, *Organometallics*, 2021, **40**, 643–653.

67 K. Nomura, I. Izawa, J. Yi, N. Nakatani, H. Aoki, H. Harakawa, T. Ina, T. Mitsudome, N. Tomotsu and S. Yamazoe, *Organometallics*, 2019, **38**, 4497–4507.

68 W. Huang, B. Li, Y. Wang, W. Zhang, L. Wang, Y. Li, W.-H. Sun and C. Redshaw, *Catal. Sci. Technol.*, 2011, **1**, 1208–1215.

69 W. Zhang and S. Luo, *Chem. Commun.*, 2022, **58**, 12979–12982.



70 W. Zhang, L. Zhang and S. Luo, *J. Am. Chem. Soc.*, 2023, **145**, 14227–14232.

71 K. Zherikova and N. Morozova, *J. Struct. Chem.*, 2012, **53**, 761–767.

72 N. Ronaghi, D. M. Fialho, C. W. Jones and S. France, *J. Org. Chem.*, 2020, **85**, 15337–15346.

73 G. Smitha, S. Patnaik and C. S. Reddy, *Synthesis*, 2005, 711–713.

74 M. Yang, Y. Guo, X. P. Zhang, H. Sun, Y. Wang, W. Zhang, Y. Wu, Y. Jian and Z. Gao, *Asian J. Org. Chem.*, 2022, **11**, e202100701.

